

Pasta Drying Modeling for Product Quality and Process Optimization

Francesco Petrosino^{a*}, Gaetano Adduci^a, Eleonora Manoli^b, Emily Cardaropoli^b, Gerardo Coppola^a, Stefano Curcio^a

^aDepartment of Computer Engineering, Modeling, Electronics and Systems (D.I.M.E.S.), Laboratory of Transport Phenomena and Biotechnology, University of Calabria, Ponte P. Bucci, Cubo 42/a, 87036 Rende (CS), Italy

^bBarilla G. e R. Fratelli S.p.A, Via Mantova 166, 43122 Parma. Italy
f.petrosino@dimes.unical.it

In the field of pasta drying, where accurate prediction of temperature and moisture content distribution is critical, the use of modeling and simulation plays a key role. This study aims to assess operational conditions that ensure the production of safe, high-quality pasta. An advanced two-domain model was developed and solved to estimate transport phenomena in both the food and air domains. Unlike traditional models that rely on predefined interfacial heat and mass transfer coefficients, the proposed model serves as a flexible tool applicable across a wide range of process and fluid-dynamic conditions in real pasta dryers. The system of nonlinear unsteady-state partial differential equations governing the behavior of a "Rigatone" pasta sample in a dryer was solved using the finite element method to evaluate how air properties affect drying performance. A pilot-scale drying chamber was used for model validation at inlet air temperatures ($T_{a,in}$) of 80 °C and relative humidity levels (RH_{in}) of 50% and 60%, with consistent errors below 10%.

1. Introduction

The production of pasta is an ancient art that has evolved over centuries, blending tradition with modern technology. From the rolling and cutting of dough to its final drying phase, each step in the process plays a critical role in determining the quality of the final product. Drying stands out as one of the most crucial stages, influencing both the sensory attributes (such as texture and flavor) and shelf life of pasta. (Guo et al., 2017).

In recent years, there has been growing interest in developing mathematical models to simulate and optimize the pasta drying process. By leveraging advanced computational tools, researchers and industry professionals are now able to predict how different drying parameters—such as temperature, humidity, air velocity, and time—affect the quality of the final product. This enables more efficient use of resources, reduced energy consumption, and improved process control (Li et al., 2019). Pasta drying modeling represents a bridge between scientific inquiry and industrial practice. By bridging this gap, new possibilities can be unlocked for innovation in the pasta industry. As consumer expectations grow increasingly sophisticated, the ability to tailor drying processes to specific product requirements becomes ever more vital. Through rigorous research and application of robust modeling techniques, manufacturers can meet these demands while maintaining cost-effectiveness and sustainability (Jamwal et al., 2020).

The complexity of pasta drying lies in its multifaceted nature, involving simultaneous changes in thermal, mechanical, and biochemical properties. For instance, improper drying conditions may lead to undesirable phenomena such as case hardening, where the outer layer dries too quickly compared to the interior, causing internal stresses and potential breakage. Similarly, insufficient drying times can result in microbial growth or spoilage due to residual moisture. To address these challenges, dynamic models capable of capturing the intricate dynamics of moisture removal and heat distribution throughout the pasta matrix have been developed (Xu et al., 2024). Another key aspect of pasta drying modeling is its contribution to process optimization. In large-scale production facilities, minimizing downtime and maximizing throughput are essential goals. Models can help identify bottlenecks in the drying process, suggest alternative configurations for dryers, and evaluate the

trade-offs associated with varying operational settings. This not only improves product consistency but also reduces waste and lowers operational costs (Shirkole et al., 2020).

Pasta drying modeling offers a powerful tool for addressing some of the most pressing issues facing the industry today, from reducing energy consumption to enhancing nutritional value. By integrating state-of-the-art modeling techniques with traditional expertise, we can pave the way for a future where high-quality pasta is produced with minimal environmental impact (Aguilar-Toalá et al., 2018; Calabuig-Jiménez et al., 2019).

The present study extends the investigation into pasta drying by introducing a novel model designed to quantify transport phenomena occurring both within the food matrix and the drying air. Unlike existing models in the literature, this framework uniquely calculates real-time interfacial transport rates, offering a flexible predictive tool adaptable to diverse process configurations and aerodynamic conditions in pasta drying systems (Adduci et al., 2024, 2025). The central objective of this research is to analyze the process optimization during pasta drying using the implemented model (Adduci et al., 2024, 2025). The goal is to refine the existing model's accuracy in predicting pasta moisture content, thereby enabling optimizations in conventional drying processes and aiding the design of novel drying protocols. This enhanced model aims to improve process efficiency while ensuring consistent high-quality product standards. The model's validation relied on a geometric configuration derived from symmetry analyses, which accounted for the three-dimensional structure of "rigatone" pasta during drying. Experimental validation was conducted using a pilot-scale drying chamber at Barilla's R&D facilities, demonstrating strong alignment with simulated results. This agreement underscores the model's reliability in replicating real-world drying dynamics.

2. Mathematical modeling

During the pasta drying process, when a cold, moist food product is exposed to a flow of hot, dry air, two primary transport phenomena occur simultaneously: heat transfer from the surrounding fluid to the solid structure of the food and the migration of moisture from the food to the drying environment. The rate at which moisture is eliminated from the food's surface depends on two factors: the diffusion of water vapor into the boundary layer formed within the drying air and the evaporation of liquid water at the food's outer surfaces (Curcio et al., 2016). The simulated case (Figure 1), is composed by the dough sample positioned centrally along the longitudinal direction of the dryer, taking on a shape and size resembling that of a "Rigatone" pasta.

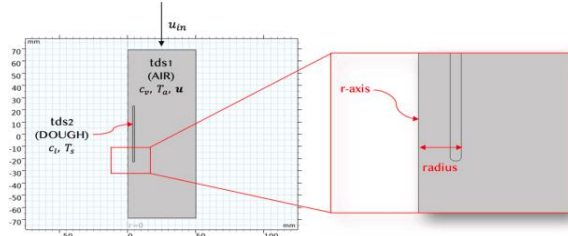


Figure 1: Model Geometry

The duct's length is three times that of the dough sample, which has a thickness of 1.3mm, a length of 46mm, and a radius of 5mm, defined as the distance of its outermost segment from the r-axis.

Therefore, modeling the pasta drying process requires an integrated approach that simultaneously addresses heat and mass transfer. The governing equations in this model link key variables such as the solid's temperature (T_s) and liquid concentration (c_l), and the fluid's temperature (T_a), vapor concentration (c_v), velocity (u), and pressure (p). These variables are connected to the thermophysical characteristics of both the food and the surrounding drying medium. The food product is treated as a non-porous medium, indeed, unlike vegetables (Curcio et al., 2016), for unleavened doughs (as in the present case), the microscopic structure of the food is more easily attributable to that of a compact solid, with porosity values below 5% and, therefore, negligible (Mercier et al. 2010). These results are in complete agreement with experimental measurements carried out by Barilla company S.p.A. (platform PL1, project "Density analysis of expanded dough for predictive model calculation PL1.4D7) where they found a porosity of the dried product equal to 4.6%.

In this framework, the model assumes that the food product undergoes mass transfer exclusively through diffusion and heat transfer solely via conduction.

Conversely, for the drying air, heat transfer occurs via convection and conduction, while water vapor transport involves both convection and diffusion. The time-dependent equations describing energy and mass transfer within the food are thus formulated using Fourier's law (Eq. 1) for heat conduction and Fick's law (Eq. 2) for mass diffusion.

$$\rho_d C_{pd} \frac{\partial T_s}{\partial t} = \nabla \cdot (k_d \nabla T_s) \quad (1)$$

$$\frac{\partial c_l}{\partial t} = \nabla \cdot (D_d \nabla c_l) \quad (2)$$

Within the framework of the proposed model, the convective component of transport equations in the food domain is neglected, based on the assumption of minimal internal evaporation. Similarly, diffusion-driven water vapor transport from the material's core to its outer surface is deemed negligible, as this mechanism is primarily relevant to highly porous materials. Instead, evaporation in this model is considered to occur predominantly at the food's outer surfaces directly exposed to the drying air (May & Perré, 2002).

The energy balance equation for the air (Eq. (3)) incorporates both convective and conductive contributions (R. Byron Bird, Warren E. Stewart, 1989; Welty, JR, Rorrer, GL, Foster, 2014).

$$\rho_a C_{pa} \frac{\partial T_a}{\partial t} - \nabla \cdot (k_a \nabla T_a) + \rho_a C_{pa} u \nabla T_a = 0 \quad (3)$$

Regarding the water mass balance within the fluid (Eq.4), taking into consideration both convective and diffusive contributions, the relevant equation is expressed as (R. Byron Bird, Warren E. Stewart, 1989; Welty, JR, Rorrer, GL, Foster, 2014).

$$\frac{\partial c_v}{\partial t} + \nabla \cdot (-D_a \nabla c_v) + u \nabla c_v = 0 \quad (4)$$

The non-isothermal air flow within the dryer, after an appropriate verification of the flow regime, has been simulated using the $k - \varepsilon$ model (Verboven et al., 1997, 2001).

The model employs a two-domain (dough-air) framework, structuring the system into two interacting domains that exchange data dynamically. It distinguishes between vapor-phase water (cv) in the fluid domain and liquid-phase water (c_l) in the pasta domain. Accordingly, mass transfer is modeled exclusively as liquid-phase transport within the solid matrix and vapor-phase transport within the fluid domain. The initial conditions are schematized in Figure 2.

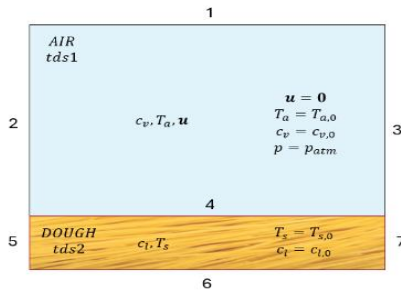


Figure 2: Schematization of the initial conditions and boundaries defined within the two domains

The boundary conditions, corresponding to the boundaries depicted in Figure 2, are summarized in Table 1.

Table 1: implemented boundary conditions

1	$u \cdot n = u_{wtr} \cdot n;$ $u_{wtr,x} = u_{in}; \quad u_{wtr,y} = 0;$ $n \cdot (-k_a \nabla T_a) = 0$ $n \cdot (-D_a \nabla c_v + c_v u) = 0$ $u_x = u_{in}; \quad u_y = 0;$ $T_a = T_{a,in} = T_{a,0}$	"Slip" condition Thermal insulation No mass flux Inlet air velocity normal to the section Inlet air temperature equal to that of the fluid domain at time $t = 0$
2	$c_v = c_{v,in} = c_{v,0}$ $p = p_{atm}$	Vapour concentration at the inlet section equal to that of fluid domain at time $t = 0$ Atmospheric pressure discharge
3	$n \cdot (-k_a \nabla T_a) = 0$ $n \cdot (-D_a \nabla c_v) = 0$ $u \cdot n = 0$ $T_a = T_s$	Convection prevailing over conduction (Heat transport) Convection prevailing over diffusion (Mass transport) "No slip" condition Temperature continuity
4	$n \cdot (-k_a \nabla T_a + \rho_a C_{pa} u \nabla T_a) =$ $n \cdot (-k_d \nabla T_s) - \lambda_{ev} n \cdot (-D_d \nabla c_l)$ $n \cdot (-D_a \nabla c_v + c_v u) = n \cdot (-D_d \nabla c_l)$ $y_v \cdot p = P_s \cdot a_w$	Heat flux continuity Mass flux continuity Thermodynamic equilibrium
5,6,7	$n \cdot (-k_d \nabla T_s) = 0$ $n \cdot (-D_d \nabla c_l) = 0$	Thermal insulation No mass flux

3. Results and discussion

Figure 3 illustrates the temperature (a) and liquid concentration (b) profiles within the solid matrix. Thermal transport within the dough layers exhibits uniformity, reflecting efficient heat conduction due to the presence of a single "Rigatone" and the minimal thickness of the dough layer. The primary thermal resistances are localized in the boundary layer adjacent to the dough, within the air domain.

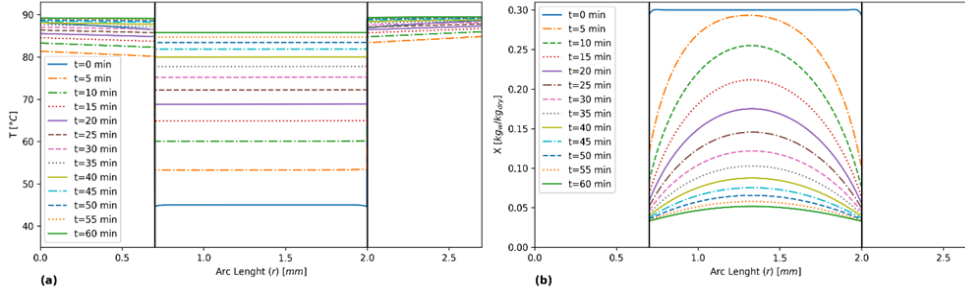


Figure 3: Radial temperature (a) and water concentration (b) at different time intervals. Vertical lines represent the sample's boundaries. ($u_{in} = 1 \frac{m}{s}$, $T_{s,0} = 45 \text{ } ^\circ\text{C}$, $RH_{in} = 30 \%$, $X_0 = 0.3 \frac{kg_w}{kg_{dry}}$)

The concentration profiles reveal a noticeable transport resistance within the sample, as expected, with distinct gradients confirming a controlled drying rate for the dough. This gradual drying strategy is intentionally employed to avoid surface layer fracturing, underscoring the necessity of avoiding harsh operational conditions during the process. Consistent with earlier observations, analyzing the boundary conditions enforcing temperature and flux continuity makes it evident that the highest heat flux occurs at the food's outer boundaries. Furthermore, the fluid mixture's temperature remains largely uniform across the domain, except for a minor localized cooling effect in the air stream directly beneath the "Rigatone." Figure 4 presents the results obtained from the parametric studies conducted on the inlet temperature of the drying air, focusing on the evolution of the average water content within the food sample on a dry basis and the average food temperature (Adduci et al., 2024, 2025).

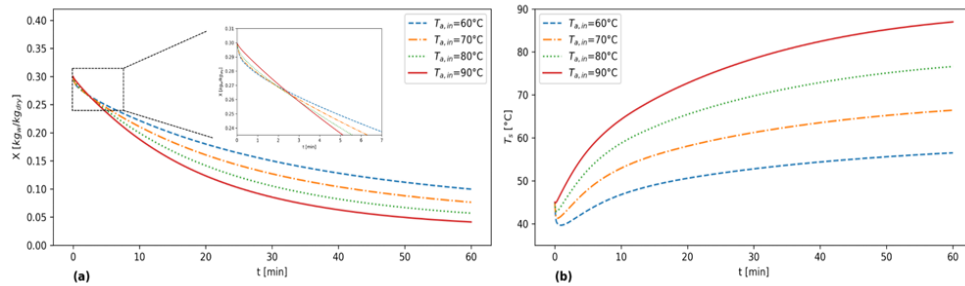


Figure 4: Evolution of the (a) moisture content on a dry basis and (b) temperature within the food after parameterization of $T_{(a,in)}$ for default configuration

As the air temperature rises, the foodstuff's moisture content is lower by the end of the drying process. However, during the initial stages of simulation, a contrasting trend is observed. With an increase in air temperature, the moisture content decreases more slowly, as the wet bulb temperature of the air-steam mixture also rises. When the temperature at the solid-fluid interface is below the wet bulb temperature of the drying medium, water vapor condenses on the sample's outer surface until its temperature equalizes with the wet bulb temperature of the fluid phase. The model was validated through drying experiments conducted in a laboratory-scale drying chamber equipped with an air temperature and relative humidity control system, a ventilation system, shelving units, a built-in scale, and a data logging and monitoring system (Italpast Test-Lab laboratory dryer EAC-LAB 60141). To recreate the structure of the model, a small amount of pasta was strategically distributed over a series of stationary perforated plates within the drying chamber. The chamber, which is approximately 50 cm high and 1m wide, was kept sealed throughout the entire drying procedure. The system was programmed to periodically halt ventilation for a few seconds to facilitate accurate measurements of the drying solid mass, ensuring accurate tracking of moisture loss. The drying process was monitored over 252 minutes under varying conditions (90°C with 40% or 60% relative humidity). Experiments were repeated in triplicate for reliability and the selected experimental conditions are representative of key stages within the industrial drying process. To account for initial disturbances caused by inserting the sample, the model incorporated transient conditions that lasted about 10 minutes before stabilizing. Comparison of model predictions with and without these transient

effects, as shown in Figure 5, demonstrated that including them improved accuracy in the early dehydration stages, though later stages remained largely unaffected. Quantitatively, the root mean square error (RMSE) values for condition (a) were 0.01 [kg_w/kg_dry] and 0.02 [kg_w/kg_dry] respectively with and without initial transient conditions; for condition (b), RMSE values were 0.02 [kg_w/kg_dry] and 0.03 [kg_w/kg_dry], respectively. These results underscore the relevance of transient phenomena primarily in the early dehydration regime. The dotted curves in Figure 5 illustrate a double change in concavity at early time points, reflecting system responses to disturbances before reaching steady-state conditions.

The model accurately described transient perturbations, though experimental data did not capture these due to measurement latency. Overall, the model predictions closely matched experimental results, with a mean relative error below 9%. Additionally, Figure 5 includes model predictions without considering glass transition phenomena, showing that incorporating this physical process significantly improves accuracy in predicting pasta dehydration. The corresponding root mean square error (RMSE) values were 0.06 [kg_w/kg_dry] for condition (a) and 0.05 [kg_w/kg_dry] for condition (b). These results further confirm that accounting for glass transition improves the model's predictive accuracy across different dehydration scenarios.

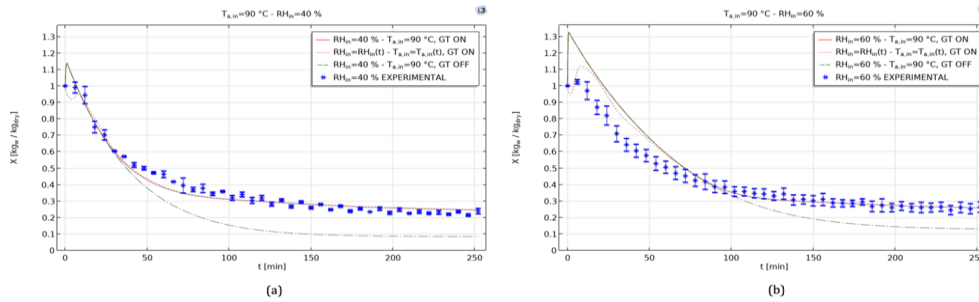


Figure 5: Comparison of experimental results and model predictions under specified drying condition ($u_{in} = 0.3$ m/s and $T_{s,0} = 30^\circ\text{C}$). Experimental points have a relative error within 10%. Model predictions are shown with transient conditions (dotted line, $T_{a,in} = T_{a,in}(t)$) and without transient conditions (solid line, $T_{a,in} = 90^\circ\text{C}$). The dash-dotted line represents model data without considering the glass transition (Adduci et al., 2025).

4. Conclusions

This paper explores the significance of pasta drying modeling in achieving high-quality products while optimizing industrial processes. For an operating temperature (T) of 90°C , results indicate a maximum heat flux (q) of approximately 290 W/m² and a final water content (X) of 4%. In an industrial context, selecting the optimal operating temperature requires balancing the shortest drying time to achieve the target moisture level with preserving product quality. While maintaining an air temperature of 90°C , a recommended practice involves reducing the drying rate by adopting gentler fluid dynamics (e.g., lower airflow velocities). This approach minimizes heat flux and mitigates risks of dough damage or structural failure during drying.

Results seamlessly reflect the experimental validation data obtained in a specifically designed drying chamber. In summary, pasta drying modeling empowers us to design smarter, greener, and more adaptable manufacturing pasta drying systems. As we delve deeper into the topics covered in this document, readers will gain valuable insights into the latest developments in this field and discover how they can apply these concepts to improve their own processes. Ultimately, the goal is to strike a balance between preserving the rich heritage of pasta-making and embracing the innovations necessary to thrive in an ever-evolving market landscape.

Nomenclature

a_w – Water activity in dough, –
 C_{pa} – Air specific heat, $J/(kg \cdot K)$
 C_{pd} – Dough specific heat, $J/(kg \cdot K)$
 c_l – Water concentration in dough, mol/m³
 c_v – Vapour concentration in air, mol/m³
 D_{eq} – Equivalent diameter of the duct, m
 D_a – Diffusion coefficient of vapour in air, m^2/s
 D_d – Diffusion coefficient of water in dough, m^2/s
 J – Interfacial mass flux, $mol / m^2 \cdot s$
 k_a – Air thermal conductivity, $W / m \cdot K$
 k_d – Dough thermal conductivity, $W / m \cdot K$

n – Unity vector normal to surface, –
 q – Interfacial heat flux, W / m^2
 P_s – Saturation pressure of water, Pa
 p – Total pressure of air-vapour mixture, Pa
 R – Gas constant, $J / mol \cdot K$
 RH – Air relative humidity, –
 r – Spatial coordinate, m
 T – Generic temperature, K
 T_a – Air temperature, K
 T_s – Dough temperature, K
 t – Time, s
 U – Dough water content wet basis, kg_w / kg_{wet}

u – Air velocity vector, m/s	λ_{ev} – Water latent heat of vaporization, J/kg
X – Dough water content dry basis, kg_w / kg_{dry}	ρ_a – Air density, kg/m^3
y_v – Vapour molar fraction in air, –	ρ_d – Dough density, kg/m^3
x, y – cartesian coordinates	in – Inlet conditions
z – Spatial coordinate, m	wb – Wet bulb conditions

Acknowledgments

The authors acknowledge the project PNRR “Tech4You” on the “Ecosistemi dell’Innovazione (ECS) of MUR (DD n.3277, December 30, 2021)” for the provided support.

References

- Adduci, G., Petrosino, F., Manoli, E., Cardaropoli, E., Coppola, G., & Curcio, S. (2024). Transport phenomena in pasta drying: a dough-air double domain advanced modeling. *Journal of Food Engineering*, 376, 112052. <https://doi.org/10.1016/J.JFOODENG.2024.112052>
- Adduci, G., Petrosino, F., Manoli, E., Cardaropoli, E., Coppola, G., & Curcio, S. (2025). Glass transition in pasta drying: Advanced modeling of the glassy layer evolution. *LWT*, 218, 117484. <https://doi.org/10.1016/J.LWT.2025.117484>
- Aguilar-Toalá, J. E., Garcia-Varela, R., Garcia, H. S., Mata-Haro, V., González-Córdova, A. F., Vallejo-Cordoba, B., & Hernández-Mendoza, A. (2018). Postbiotics: An evolving term within the functional foods field. *Trends in Food Science & Technology*, 75, 105–114. <https://doi.org/10.1016/J.TIFS.2018.03.009>
- Calabuig-Jiménez, L., Betoret, E., Betoret, N., Patrignani, F., Barrera, C., Seguí, L., Lanciotti, R., & Dalla Rosa, M. (2019). High pressures homogenization (HPH) to microencapsulate *L. salivarius* spp. *salivarius* in mandarin juice. Probiotic survival and in vitro digestion. *Journal of Food Engineering*, 240, 43–48. <https://doi.org/10.1016/J.JFOODENG.2018.07.012>
- Curcio, S., Aversa, M., Chakraborty, S., Calabrò, V., & Iorio, G. (2016). Formulation of a 3D conjugated multiphase transport model to predict drying process behavior of irregular-shaped vegetables. *Journal of Food Engineering*, 176, 36–55. <https://doi.org/https://doi.org/10.1016/j.jfoodeng.2015.11.020>
- Guo, X. fei, Yang, B., Cai, W., & Li, D. (2017). Effect of sea buckthorn (*Hippophae rhamnoides* L.) on blood lipid profiles: A systematic review and meta-analysis from 11 independent randomized controlled trials. *Trends in Food Science & Technology*, 61, 1–10. <https://doi.org/10.1016/J.TIFS.2016.11.007>
- Jamwal, R., Amit, Kumari, S., Balan, B., Dhaulaniya, A. S., Kelly, S., Cannavan, A., & Singh, D. K. (2020). Attenuated total Reflectance–Fourier transform infrared (ATR–FTIR) spectroscopy coupled with chemometrics for rapid detection of argemone oil adulteration in mustard oil. *LWT*, 120, 108945. <https://doi.org/10.1016/J.LWT.2019.108945>
- Li, K., Liu, J. Y., Fu, L., Li, W. J., Zhao, Y. Y., Bai, Y. H., & Kang, Z. L. (2019). Effect of gellan gum on functional properties of low-fat chicken meat batters. *Journal of Texture Studies*, 50(2), 131–138. <https://doi.org/10.1111/JTXS.12379>
- May, B. K., & Perré, P. (2002). The importance of considering exchange surface area reduction to exhibit a constant drying flux period in foodstuffs. *Journal of Food Engineering*, 54(4), 271–282. [https://doi.org/https://doi.org/10.1016/S0260-8774\(01\)00213-8](https://doi.org/https://doi.org/10.1016/S0260-8774(01)00213-8)
- R. Byron Bird, Warren E. Stewart, E. N. (1989). R. Byron Bird, Warren E. Stewart, Edwin N. Lightfoot - Transport Phenomena, 2nd Edition-Wiley (2001). In *Arquivos brasileiros de cardiologia* (Vol. 52, Issue 3).
- Shirkole, S. S., Jayabalan, R., & Sutar, P. P. (2020). Dry Sterilization of Paprika (*Capsicum annum* L.) by Short Time-Intensive Microwave-Infrared Radiation: Establishment of Process Using Glass Transition, Sorption, and Quality Degradation Kinetic Parameters. *Innovative Food Science & Emerging Technologies*, 62, 102345. <https://doi.org/10.1016/J.IFSET.2020.102345>
- Verboven, P., Nicolaï, B. M., Scheerlinck, N., & De Baerdemaeker, J. (1997). The local surface heat transfer coefficient in thermal food process calculations: A CFD approach. *Journal of Food Engineering*, 33(1), 15–35. [https://doi.org/https://doi.org/10.1016/S0260-8774\(97\)00041-1](https://doi.org/https://doi.org/10.1016/S0260-8774(97)00041-1)
- Verboven, P., Scheerlinck, N., De Baerdemaeker, J., & Nicolaï, B. M. (2001). Sensitivity of the food centre temperature with respect to the air velocity and the turbulence kinetic energy. *Journal of Food Engineering*, 48(1), 53–60. [https://doi.org/10.1016/S0260-8774\(00\)00145-X](https://doi.org/10.1016/S0260-8774(00)00145-X)
- Welty, JR, Rorrer, GL, Foster, D. (2014). *Fundamentals of Momentum, Heat, and Mass Transfer*, 6th Ed. In John Wiley & Sons.
- Xu, Z., Han, S., Guan, S., Zhang, R., Chen, H., Zhang, L., Han, L., Tan, Z., Du, M., & Li, T. (2024). Preparation, design, identification and application of self-assembly peptides from seafood: A review. *Food Chemistry: X*, 23, 101557. <https://doi.org/10.1016/J.FOCHX.2024.101557>